

Formation of Nanoneedles and Nanoplatelets of KNbO_3 Perovskite during Templated Crystallization of the Precursor Gel

Irena Pribošič^{*,†} Darko Makovec[†] and Miha Drofenik^{†,‡}

Jožef Stefan Institute, Jamova 39, SI-1000 Ljubljana, Slovenia, and Faculty of Chemistry and Chemical Engineering, University of Maribor, Smetanova 17, SI-2000 Maribor, Slovenia

Received January 13, 2005. Revised Manuscript Received March 23, 2005

Highly anisotropic nanocrystallites in the form of nanoneedles and nanoplatelets of KNbO_3 perovskite were prepared by crystallization of the amorphous gel. The gel was prepared by the polymerizable-complex method based on the Pechini-type reaction route. The nanoneedles were typically 50 nm thick and approximately 10 μm long and had surfaces parallel to the $\{100\}$ planes of the pseudocubic perovskite. The formation of these pseudocubic KNbO_3 perovskite crystallites of an unusual and highly anisotropic shape was studied by electron microscopy in combination with X-ray diffractometry and thermal analyses. A layer-structured compound, $\text{K}_4\text{Nb}_6\text{O}_{17}$, appeared as the first crystalline phase during the heating of the amorphous precursor gel at temperatures around 490 °C. When this compound reacts to form the cubic perovskite at higher temperatures (around 540 °C), its highly anisotropic, layered structure defines the anisotropic shape of the product.

Introduction

Tailoring the shape of a material on the nanometer scale is one of the key problems in nanotechnology. Normally, the shape of crystalline particles depends on their internal structure. This means that materials with a cubic structure will normally form isotropic particles, for example, cubes or octahedra. To modify the shape of particles with a cubic structure, it is necessary to apply special methods. In this work we studied the formation of highly anisotropic nanocrystallites in the form of nanoneedles and nanoplatelets of pseudocubic KNbO_3 during crystallization of the precursor gel obtained by a polymerized complex (PC) method.

Potassium niobate (KNbO_3) belongs to a technologically important group of perovskite materials. In the past few years, KNbO_3 and its solid solutions have been widely studied because of their high-temperature ferroelectricity and piezoelectricity and in particular because these materials do not contain poisonous lead, which is still used in standard high-performance piezoelectric materials (e.g., lead zirconium titanate, PZT). Recently, there has been a report of high-performance lead-free piezoceramics based on $(\text{K},\text{Na})\text{NbO}_3$ being prepared.¹ Ceramics based on KNbO_3 were also tested as lead-free materials with a positive temperature coefficient of resistivity (PTCR).^{2,3} Furthermore, KNbO_3 is one of the most promising materials for nonlinear optical and electrooptical devices because of its large nonlinear susceptibility and high photorefractive coefficient.⁴

The synthesis of KNbO_3 -based material by solid-state reaction techniques is difficult due to the large differences in the properties of the cations involved. However, various wet chemical methods have been reported for the preparation of KNbO_3 , ranging from hydrothermal^{5–8} and glycothermal methods⁹ to sol–gel^{10,11} and the PC method.^{12,13} The PC method is based on the Pechini-type reaction route,¹⁴ starting from a precursor solution of the respective metal–citrate complexes. The metal–citrate complexes react with ethylene glycol in an esterification reaction, forming a homogeneous gel. KNbO_3 is obtained by crystallization of the precursor gel at temperatures around 600 °C.

Experimental Procedures

Niobium(V) chloride (NbCl_5 , Alfa 51108), potassium carbonate (K_2CO_3 , Aldrich 20,961-9), citric acid (CA) ($\text{C}_6\text{O}_7\text{H}_8$, Alfa 31185), and ethylene glycol (EG) ($\text{C}_2\text{O}_2\text{H}_6$, Alfa 31332) were used to synthesize the KNbO_3 (KN) powders. A schematic of the experimental procedure is illustrated in Figure 1.

For the preparation of the powders, CA (0.3 mol) and NbCl_5 (0.01 mol) were dissolved in 100 mL and 50 mL of methanol (MeOH), respectively. With continuous stirring, the NbCl_5 solution was slowly added to the solution of CA. K_2CO_3 (0.005 mol) powder was added and the solution was magnetically stirred for 1 h to obtain

* Corresponding author: tel +386-1-477-3762; fax +386-1-477-3875; e-mail irena.pribosic@ijs.si.

[†] Jožef Stefan Institute.

[‡] University of Maribor.

- (1) Saito, Y.; Takao, H.; Tani, T.; Nonoyama, T.; Takatori, K.; Homma, T.; Nagaya, T.; Nakamura, M. *Nature* **2004**, *432*, 84.
- (2) Pribošič, I.; Makovec, D.; Drofenik, M. In *Proceedings of the 7th Conference of the ECERS*; Brugge, Belgium, 2001; Vol. 2, p 1401.
- (3) Pribošič, I.; Makovec, D.; Drofenik, M. *J. Mater. Res.* **2002**, *17*, 2989.
- (4) Xue, D.; Zhang, S. *Chem. Phys. Lett.* **1998**, *291*, 401.

- (5) Kormamneni, S.; Roy, R.; Li, Q. H. *Mater. Res. Bull.* **1992**, *27*, 1393.
- (6) Lu, C. H.; Lo, S. Y.; Lin, H. C. *Mater. Lett.* **1998**, *34*, 172.
- (7) Uchida, S.; Inoue, Y.; Fujishiro, Y.; Sato, T. *J. Mater. Sci.* **1998**, *33*, 5125.
- (8) Goh, G. K. L.; Lange, F. F. *J. Mater. Res.* **2003**, *18*, 338.
- (9) Lu, C. H.; Lo, S. Y.; Wang, Y. L. *Mater. Lett.* **2002**, *55*, 121.
- (10) Nazeri-Eshghi, A.; Kuang, A. X.; Mackenzie, J. D. *J. Mater. Sci.* **1990**, *25*, 3333.
- (11) Amini, M. M.; Sacks, M. D. *J. Am. Ceram. Soc.* **1991**, *74*, 53.
- (12) Pribošič, I.; Makovec, D.; Drofenik, M. *J. Eur. Ceram. Soc.* (special issue, in press).
- (13) Simoes, A. Z.; Ries, A.; Riccardi, C. S.; Gonzalez, A. H.; Zaghet, M. A.; Stojanovic, B. D.; Cilense, M.; Varela, J. A. *Mater. Lett.* **2004**, *58*, 2537.
- (14) Pechini, M. P. U.S. Patent 3,330,697, 1967.

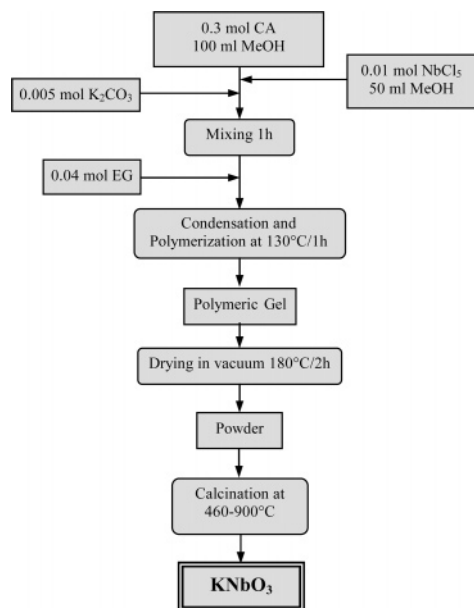


Figure 1. Flow diagram for preparing KNbO_3 by the PC method.

a clear, colorless solution of metal–citrate complexes. This solution, containing Nb^{5+} and K^+ cations, was mixed with 0.04 mol of EG. The mixture was then slowly heated to 130 °C for 1 h, first to evaporate the methanol and subsequently to promote esterification between the CA and the EG. During condensation of the solution, white precipitates were formed, but the solid substance was dissolved when the temperature reached 130 °C. After esterification, a clear, slightly yellow polymeric gel appeared. This gel remained clear after cooling to room temperature. Drying the resin in a vacuum at 180 °C for 2 h resulted in a dark yellow, solid precursor.

Later, the precursors were calcinated at temperatures from 460 to 900 °C in a flow of air. The thermal decomposition and crystallization of the precursor were investigated by thermogravimetry and differential thermal analysis (TGA-DTA, Netzsch, STA 409) in a flow of air (45 mL/min) at a heating rate of 0.2 °C/min, X-ray powder diffraction (model D4 Endeavor, Bruker AXS), and field-emission electron-source scanning electron microscopy, FES-EM (SUPRA 35 VP, Carl Zeiss). For TEM investigations the calcined powders were deposited on a copper-grid-supported transparent carbon foil. The samples were examined by a field-emission electron-source scanning-transmission electron microscope (STEM; JEOL 2010 F), operated at 200 kV. The microscope is equipped with an energy-dispersive microanalysis system (EDS; LINK ISIS EDS 300).

Results and Discussion

Figure 2 shows the TGA/DTA curves obtained during slow heating (heating rate 0.2 °C/min) of the precursor gel obtained by the PC method. Prior to the analysis, the precursor gel was dried at 280 °C. The DTA curve shows four partially overlapping exothermic events at temperatures around 285, 380, 490, and 540 °C. From the TGA curve we can see that the four exothermic events are associated with weight losses of 48.9%, 33.3%, 5.3%, and 4.5%, respectively. The first and second peaks in the DTA curve, both associated with a large weight loss, can be related to the burnout of organic species contained in the precursor gel. To determine the nature of the third and fourth exothermic events, we used X-ray diffraction (XRD) analysis (Figure 3). For this experiment, KNbO_3 powder precursors were heated to 460,

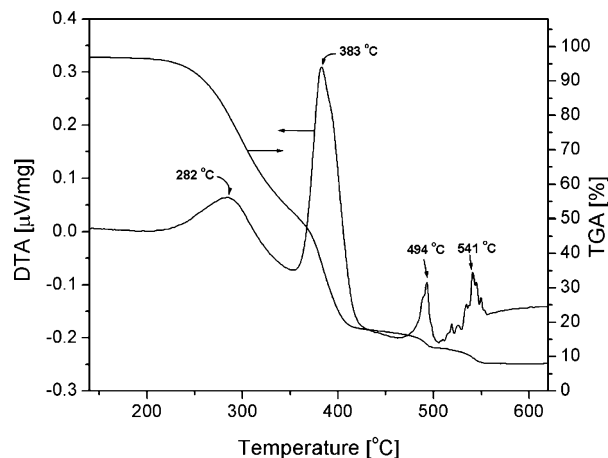


Figure 2. TGA/DTA curves of the PC precursor gel heated at a rate of 0.2 °C/min in a flow of air (45 mL/min). Prior to the analysis, the precursor gel was dried at 280 °C.

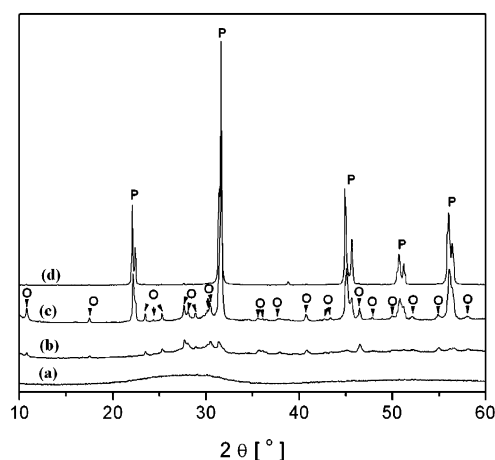


Figure 3. XRD patterns of PC precursor gel heated to (a) 460, (b) 510, (c) 560, and (d) 900 °C at a heating rate of 0.2 °C/min. Peaks marked O correspond to the structure of $\text{K}_4\text{Nb}_6\text{O}_{17}$, whereas peaks marked P match with the KNbO_3 perovskite structure.

510, 560, and 900 °C, with the same heating rate of 0.2 °C/min that was used for the TG/DT analysis. The X-ray diffraction pattern of the powder that was slowly heated to 460 °C (Figure 3a) indicates no crystalline structure can be detected. The XRD spectrum of the powder that was slowly heated to 510 °C (Figure 3b) shows the presence of reflections that could be ascribed to the crystalline phase $\text{K}_4\text{Nb}_6\text{O}_{17}$ [K_4N_6 orthorhombic; $a = 0.7830$ nm, $b = 3.321$ nm, $c = 0.6460$ nm; space group $\text{P2}_1\text{nb}(33)$].¹⁵ Thus, the third, small peak in the DTA/TGA curves around 494 °C is most probably related to the crystallization of K_4N_6 . The XRD pattern of the sample slowly heated to 560 °C shows, besides the peaks of the K_4N_6 phase, strong peaks corresponding to the KNbO_3 perovskite [KN orthorhombic; $a = 0.3971$ nm, $b = 0.5697$ nm, $c = 0.5723$ nm; space group $\text{Amm}2(38)$].¹⁶ With a further increase in temperature or a longer time at a temperature above ~540 °C, the amount of K_4N_6 phase decreased while the amount of KN phase increased. After calcination at 900 °C (Figure 3d), only the KN compound was present. The cell parameters of the

(15) Gasperin, M.; Le Bihan, M. T. *J. Solid State Chem.* **1982**, *43*, 346.

(16) Shuvaeva, V. A.; Antipin, M. Y. *Kristallografiya* **1995**, *40*, 511.

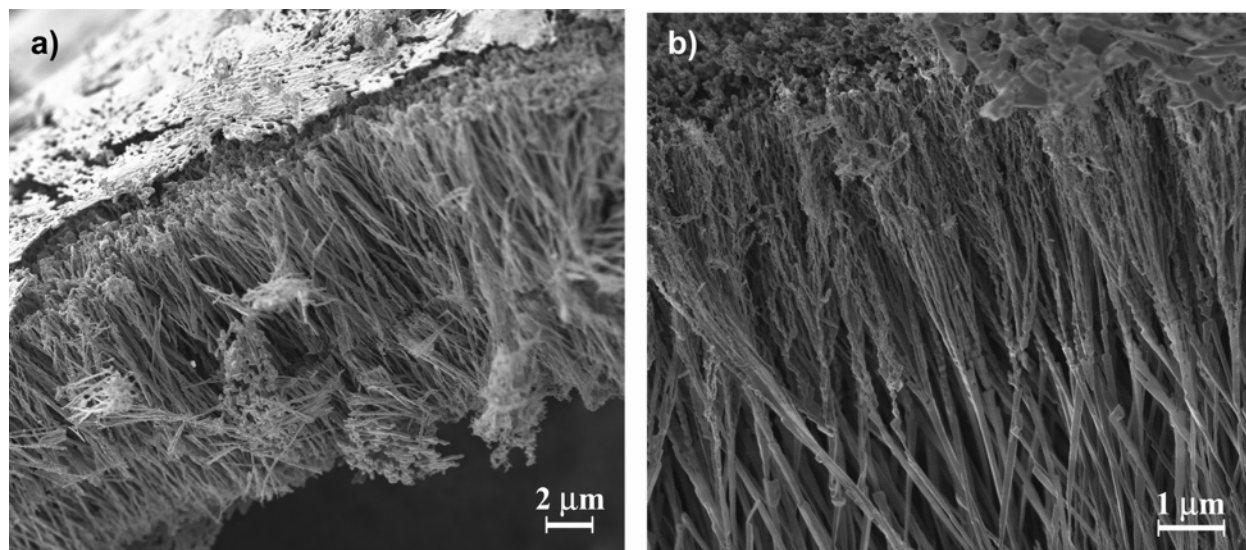


Figure 4. SEM images of the KN particles prepared by calcination of the PC precursor gel at 540 °C for 1 h: (a) typical agglomerate of KN nanoneedles with KN nanoplatelets at the top; (b) high-magnification image, showing the branching of the nanoneedles.

orthorhombic KN were determined to be $a = 0.5696$ nm, $b = 0.5709$ nm, and $c = 0.3983$ nm, which is close to those reported for that compound.¹⁶ The XRD analysis proved that the fourth peak in the DTA curve at around 540 °C is related to the crystallization of KN. Above 560 °C, no further weight loss or thermal effects could be detected by TGA/DTA up to 800 °C.

The results show that the crystallization of the KN occurs in two stages. In the first stage the K_4N_6 crystallizes from an amorphous precursor and subsequently reacts to form KN in the second stage. Because the composition of K_4N_6 is potassium-deficient with respect to the composition of KN, the presence of a potassium-rich phase is expected in the sample heated to 510 °C. However, no such phase was visible on the X-ray diffraction pattern (Figure 3b), most probably because it is not present as a separate crystalline phase.

Figure 4 shows SEM images of the particles prepared by the calcination of the PC precursor gel at 540 °C for 1 h. The sample consisted of agglomerates of nanoneedles (nanowires), approximately 10 μm long, usually extending between wide platelets. It is evident from the XRD analysis of the sample that those nanoparticles are formed from KN. The overall shape of the agglomerates was platelike; these plates had thicknesses of about 20 μm and lengths in the range of a few hundred micrometers. An agglomerate is shown in Figure 4a; the nanoneedles are clearly visible, with the platelets to the top of the agglomerate. Figure 4b is a high-magnification image, showing the parallel nanoneedles below the platelet surface and evidence for needle branching as the needles extend toward the upper platelet surface.

Figure 5 shows a TEM image of the nanoneedles and nanoplatelets from the same sample as shown in Figure 4 (prepared by calcination of the precursor gel at 540 °C for 1 h). Electron diffraction patterns taken from both the nanoneedles and the nanoplatelets matched with the perovskite KN structure. Figure 6 shows a high-resolution electron microscopic (HREM) image and a corresponding electron diffraction pattern of the nanoneedle, oriented along the $\langle 100 \rangle$ direction of the perovskite's pseudocubic structure. The

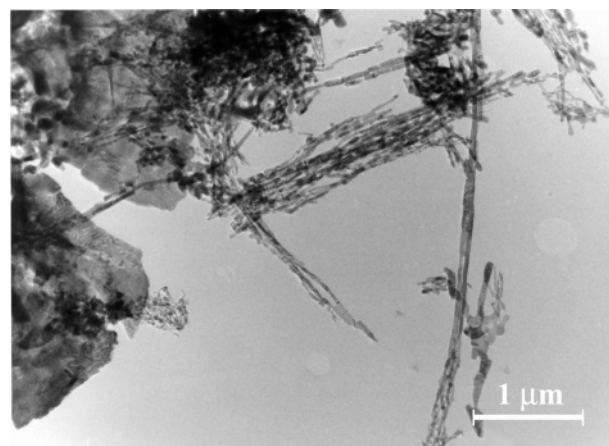


Figure 5. TEM image of highly anisotropic KNbO_3 particles prepared by calcination of the PC precursor gel at 540 °C for 1 h.

nanoneedle is fully crystalline, with surfaces parallel to the perovskite's $\{100\}$ planes. Also, the extensive surfaces of the nanoplatelets were found to be parallel with the perovskite's $\{100\}$ planes.

The nanoplatelets were approximately 50 nm thick (measured from SEM images) and up to several tens of micrometers wide. Also, the extensive surfaces of the nanoplatelets were found to be parallel to the perovskite's $\{100\}$ planes. The platelets frequently branched into a number of nanorods, as shown in Figure 7.

At the crystallization temperature KNbO_3 has a cubic structure. An isotropic cubic structure normally leads to the formation of isotropic crystallites, mostly cubic or octahedral. The formation of anisotropic crystallites in the form of nanoneedles and nanoplatelets of cubic material is very unusual. In our study we followed the hypothesis that the formation of anisotropic perovskite crystallites during the heating of the PC precursor gel is related to the fact that the crystallization of perovskite does not occur directly from the amorphous precursor but through an intermediate crystalline phase. This intermediate phase influences the shape of the perovskite crystallites. By use of XRD analyses, K_4N_6 was

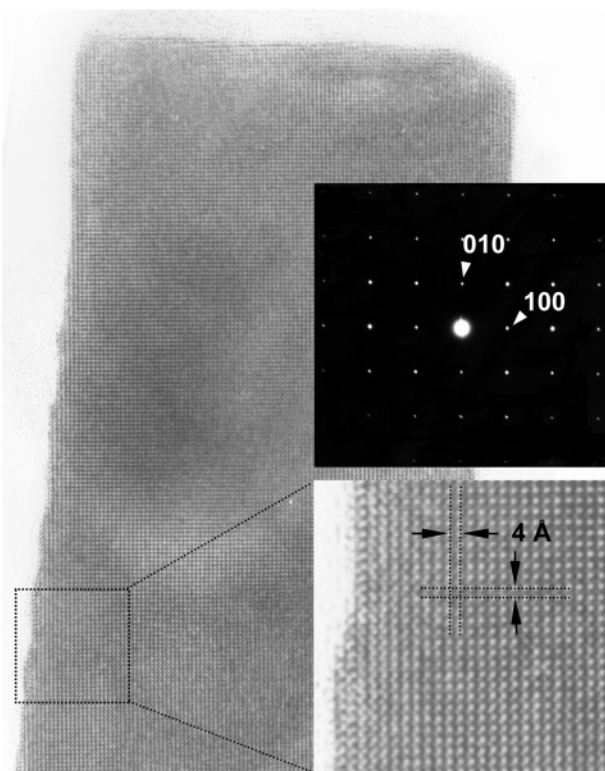


Figure 6. HREM image and corresponding electron diffraction pattern (inset) of the KNbO_3 nanoneedle. The sample was prepared by calcination of the PC precursor gel at 540°C for 1 h.

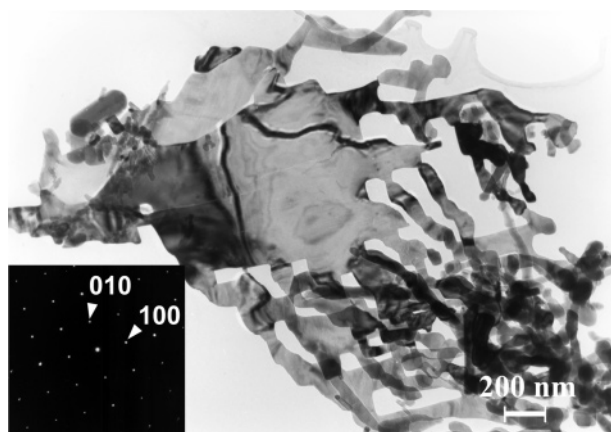


Figure 7. TEM image and corresponding electron diffraction pattern (inset) of a branched nanoplatelet of the KNbO_3 perovskite in the sample prepared by calcination of the PC precursor gel at 540°C for 1 h.

detected as the first crystalline phase to form during heating of the amorphous precursor.

TEM analysis of the sample prepared by the calcination of the precursor gel for 1 h at 460°C showed that the majority of the sample consists of large (few micrometers) amorphous particles with no particular shape, and embedded in the amorphous matrix there were a few regions of poorly crystalline material. The crystalline areas had the shape of elongated platelets, and their structure was very sensitive to the electron beam.

In the sample prepared by the calcination of the amorphous precursor gel for 1 h at 510°C , individual platelike crystallites of $\text{K}_4\text{Nb}_6\text{O}_{17}$ and some highly anisotropic perovskite nanocrystallites were observed. However, the majority of the material consisted of the poorly crystalline, elongated plate-

like particles. Electron diffraction patterns of those particles were identical to the electron diffraction patterns of the first, poorly crystalline phase observed in the sample calcined at 460°C . Figure 8 shows a bright field (BF) image of such an elongated platelike particle (Figure 8a) and the corresponding electron diffraction pattern (Figure 8b). The contrast of the BF image of the particle is uneven, with alternating dark and bright areas. An EDS analysis of the particle showed that it contained K and Nb at a ratio of approximately 4:6. The corresponding electron diffraction pattern (Figure 8b) is characterized by a middle row of relatively sharp reflections perpendicular to the elongation of the particle, whereas the rows of reflections parallel to the middle row are diffuse and streaked. When the platelet was tilted in the TEM, the basic features of the electron diffraction pattern remained almost unchanged.

The electron diffraction pattern of the elongated platelet particles could be indexed on the basis of a layered structure of K_4N_6 .

The structure of K_4N_6 (Figure 9) could be represented as a stacking of $(-\text{Nb}_6\text{O}_{17}-)$ sheets composed of corner-sharing and edge-sharing (NbO_6) octahedra.¹⁵ The orthorhombic unit cell of K_4N_6 consists of four $(-\text{Nb}_6\text{O}_{17}-)$ sheets stacked along the b direction of the cell. Each sheet consists of a layer of (NbO_6) octahedra sharing corners along the $[100]$ direction and alternately sharing corners and edges along the $[001]$ direction. On the top and bottom of this layer, the rest of the (NbO_6) octahedra are bonded. The potassium atoms are situated at the top and bottom of the sheet. The chemical bonds inside the sheet are much stronger than between the sheets. Each individual sheet has a different atomic density at its top compared to its bottom, giving it inherent mechanical strain. It was shown by Saupe et al.¹⁷ that when the K_4N_6 crystal is exfoliated into individual sheets, they spontaneously curl into tubules.

The diffraction pattern (Figure 8b) typical for the poorly crystalline elongated platelets, which appeared as the first crystalline phase during the heating of the amorphous precursor, could be explained by curling of the $\text{K}_4\text{Nb}_6\text{O}_{17}$ sheets. The electron diffraction pattern is basically a superimposition of the two diffraction patterns of the $\text{K}_4\text{Nb}_6\text{O}_{17}$ structure along the $[010]$ direction, which are rotated away from each other (marked in Figure 8b), and of the row of (040) reflections. The periodicity of the (040) reflections is related to the individual $(-\text{Nb}_6\text{O}_{17}-)$ sheet. Such a pattern would be typical for nanotubes formed by curling of the $\text{K}_4\text{Nb}_6\text{O}_{17}$ sheets around the $[101]$ direction (marked in Figure 9b). However, the shape of the platelet particles (Figure 8a) does not agree with the assumption that they are nanotubes. It could be concluded that the platelets are composed of the strongly curled $\text{K}_4\text{Nb}_6\text{O}_{17}$ sheets, which at least locally form tubules or scrolls. Usually, individual reflections coming from other $\text{K}_4\text{Nb}_6\text{O}_{17}$ zone axes, for example $[101]$, are also present in the complex diffraction pattern of the platelet particle.

HREM imaging of those particles of curled $\text{K}_4\text{Nb}_6\text{O}_{17}$ sheets was very difficult due to their high sensitivity to the

(17) Saupe, G. B.; Waraksa, C. C.; Kim, H.-N.; Han, Y. J.; Kaschak, D. M.; Skinner, D. M.; Mallouk, T. E. *Chem. Mater.* **2000**, *12*, 1556.

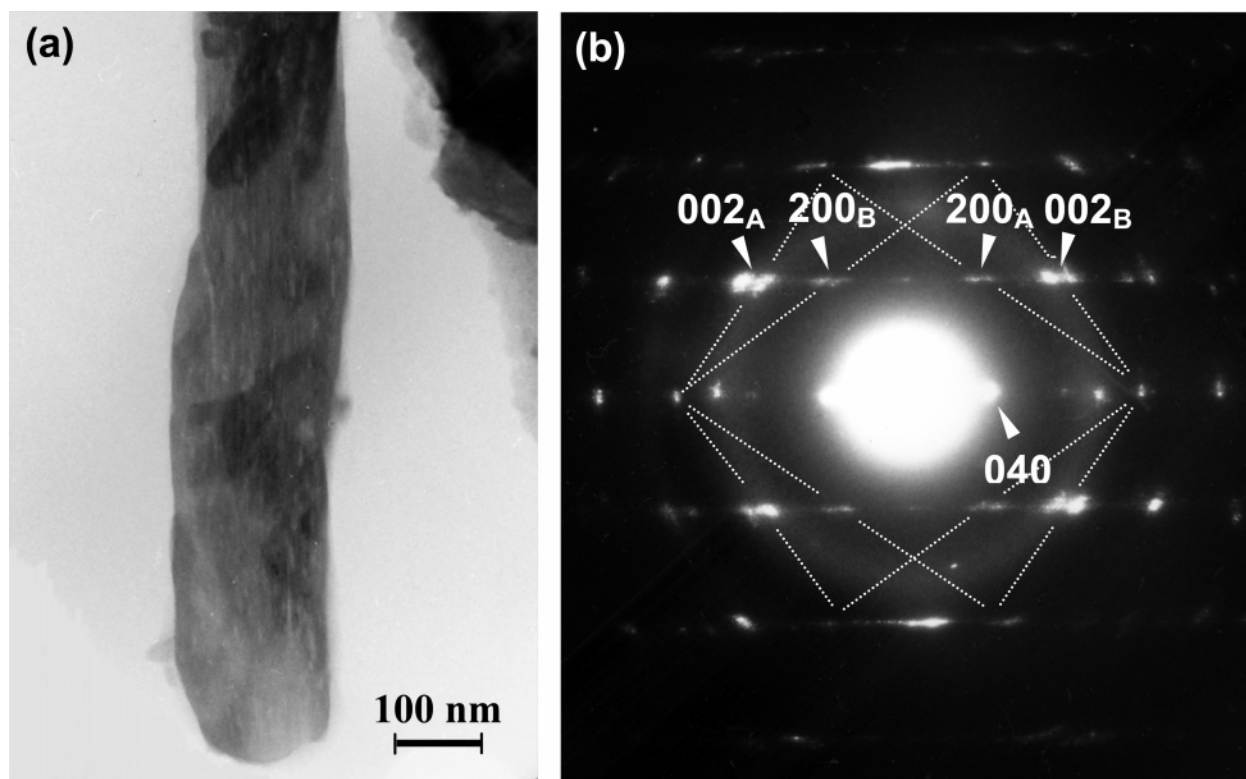


Figure 8. (a) BF image and (b) corresponding electron diffraction pattern of the poorly crystalline, elongated platelike particle. The sample was prepared by calcination of the PC precursor gel at 510 °C for 1 h.

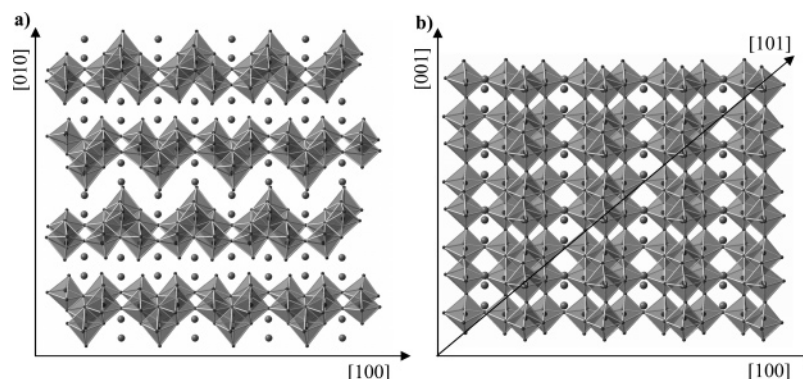


Figure 9. Schematic representation of the structure of $\text{K}_4\text{Nb}_6\text{O}_{17}$ along (a) the $[001]$ direction and (b) the $[010]$ direction.

electron beam. Even a brief irradiation of the particles caused their partial amorphization, and sometimes, with intensive irradiation, the particles of curled $\text{K}_4\text{Nb}_6\text{O}_{17}$ sheets transformed into a new structure. Figure 10 shows the sequence of the electron diffraction patterns taken during irradiation of the platelike particle with the electron beam. Before the irradiation, the electron diffraction pattern of the particle agreed with its structure being composed of curled $\text{K}_4\text{Nb}_6\text{O}_{17}$ sheets (Figure 10a). The diffraction pattern in Figure 10b was taken after a brief irradiation with the intensive electron beam. The majority of the reflections characteristic of curled $\text{K}_4\text{Nb}_6\text{O}_{17}$ sheets almost completely disappeared, while the diffuse reflections corresponding to one of the original $[010]$ zone patterns of the $\text{K}_4\text{Nb}_6\text{O}_{17}$ structure remained bright (marked in Figure 10a,b). Due to the irradiation with the electron beam, which caused heating of the particle, the originally curled $\text{K}_4\text{Nb}_6\text{O}_{17}$ sheets obviously locally uncurled and straightened parallel to the specimen's carbon support.

After a longer irradiation the $\text{K}_4\text{Nb}_6\text{O}_{17}$ transformed into the new structure. Figure 10c shows the corresponding diffraction pattern, which matches with a pseudocubic perovskite structure along the $[010]$ direction. The $\{200\}$ reflections of the original orthorhombic $\text{K}_4\text{Nb}_6\text{O}_{17}$ structure (marked O in Figure 10a,b) coincide with the $\{100\}$ reflections of the perovskite (P) structure.

The transformation of the orthorhombic $\text{K}_4\text{Nb}_6\text{O}_{17}$ material into a pseudocubic perovskite, observed during the irradiation of the material in TEM, strongly supports the idea that the perovskite KNbO_3 is obtained by crystallization through the layer-structured $\text{K}_4\text{Nb}_6\text{O}_{17}$ phase.

The first, poorly crystalline, elongated, platelike particles composed of curled $\text{K}_4\text{Nb}_6\text{O}_{17}$ sheets were already observed after the amorphous precursor was heated for 1 h at 460 °C. The DT/TG analyses combined with the XRD showed the crystallization of $\text{K}_4\text{Nb}_6\text{O}_{17}$ occurring at around 490 °C, when the precursor was continuously heated at a rate of 0.2 °C/

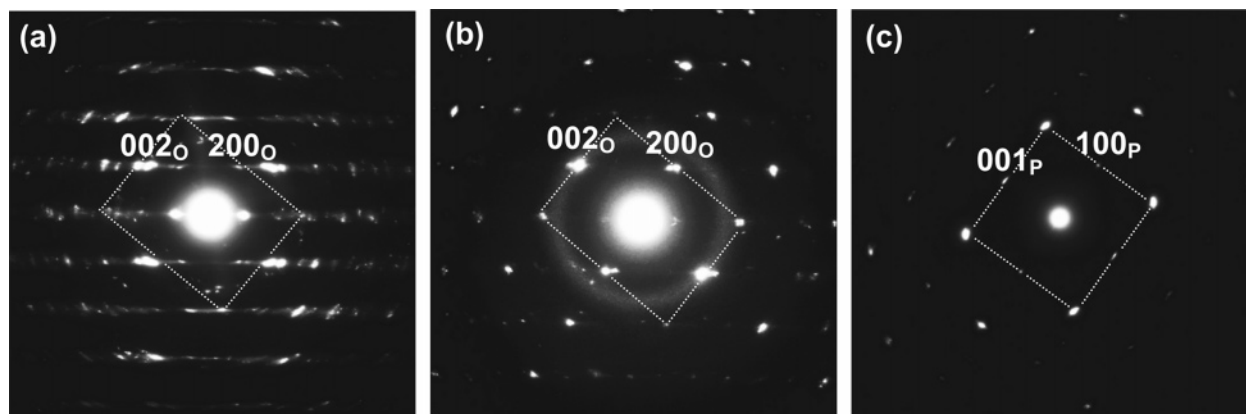


Figure 10. Sequence of electron diffraction patterns taken during irradiation of a particle composed of strongly curled $\text{K}_4\text{Nb}_6\text{O}_{17}$ sheets with the electron beam: (a) before irradiation, (b) after a short irradiation, and (c) after a longer intensive irradiation.

min. During the crystallization of the perovskite, the $\text{K}_4\text{Nb}_6\text{O}_{17}$ sheets served as templates. Compared to the KNbO_3 perovskite, the $\text{K}_4\text{Nb}_6\text{O}_{17}$ has a composition deficient in terms of K_2O . Thus, for the chemical reaction of KNbO_3 formation, potassium needs to diffuse inside the $\text{K}_4\text{Nb}_6\text{O}_{17}$ template. Due to its layered structure, with weak bonds between the $\text{K}_4\text{Nb}_6\text{O}_{17}$ sheets, the diffusion of potassium into the template should be fast. It is known that $\text{K}_4\text{Nb}_6\text{O}_{17}$ has a strong tendency to form intercalates.¹⁵ The anisotropic structure of the $\text{K}_4\text{Nb}_6\text{O}_{17}$ template influences the shape of the finally formed perovskite. Each individual $\text{K}_4\text{Nb}_6\text{O}_{17}$ sheet of the $\text{K}_4\text{Nb}_6\text{O}_{17}$ structure is anisotropic: the stacking of (NbO_6) octahedra is different in the $[100]$ direction than in the $[001]$ direction. The sheet consists of a central layer of (NbO_6) octahedra, with shear corners in the $[100]$ direction and alternating edges and corners in the $[001]$ direction (Figure 9). The corner-shearing (NbO_6) octahedra are also an inherent structural feature of the perovskite structure. On the basis of the transformation from $\text{K}_4\text{Nb}_6\text{O}_{17}$ to perovskite observed during irradiation with the electron beam in the TEM, it could be concluded that those corner-sharing octahedra extending in the $[100]$ direction of the $\text{K}_4\text{Nb}_6\text{O}_{17}$ (Figure 9) also remain in the finally formed perovskite; they form the backbone of the structure of the formed perovskite. The majority of the perovskite particles templated by the $\text{K}_4\text{Nb}_6\text{O}_{17}$ sheets had the shape of nanoneedles; however, some of the particles also had the shape of thin platelets (Figure 4). The facets of those anisotropic perovskite particles were parallel to the $\{100\}$ planes of the pseudocubic structure.

Seno and Tani¹⁸ studied the structural transformation from a layered-perovskite $\text{Bi}_4\text{Ti}_3\text{O}_{12}$ template to a regular perovskite $\text{Bi}_{0.5}(\text{Na}_{0.87}\text{K}_{0.13})_{0.5}\text{TiO}_3$ product during an in situ, high-temperature chemical reaction using a TEM. In this case, a close similarity exists between the structure of the template and the finally formed product, while compositionally the template showed some differences in comparison to the product. The reaction started within the surface region of the template and proceeded toward its inner part. The reaction can be regarded as topotactic, and during the reaction the template itself changed its structure.

Templated crystallization is a helpful tool for the synthesis of highly anisotropic nanoparticles of cubic materials. The

anisotropic particles of the KNbO_3 -based material could be technologically important, for example, in the processing of lead-free piezoelectric ceramics. It is known that piezoelectric ceramics with a textured microstructure have superior properties to ceramics with randomly oriented grains.¹ However, the texturing of the grains of basically cubic material, such as perovskites, is difficult. It cannot be achieved by "classical" methods, for example, by hot pressing.¹⁹ However, textured ceramics can be prepared by orientation of the anisotropic particles of KNbO_3 , synthesized with templated crystallization. Tape casting has been successfully used for the texturing of anisotropic grains.²⁰ Alternatively, textured KNbO_3 -based ceramics can be prepared by using $\text{K}_4\text{Nb}_6\text{O}_{17}$ as a template for reactive-templated grain growth (RTGG). RTGG is based on the orientation of the template particles with a highly anisotropic shape (e.g., $\text{K}_4\text{Nb}_6\text{O}_{17}$) in a mixture of other components (K_2CO_3) needed for the final product (KNbO_3). After the reaction, the grains of product adopt the orientation of the template.^{21–24}

Conclusions

Nanoneedles and nanoplatelets of KNbO_3 were synthesized by the polymerized complex (PC) method. The unusual, highly anisotropic shape of the nanocrystallites with a pseudocubic perovskite structure was found to be a result of the templated crystallization. During calcination of the amorphous gel, a $\text{K}_4\text{Nb}_6\text{O}_{17}$ compound crystallizes first. Subsequently, this compound reacts to form KNbO_3 perovskite in a chemical reaction in which the highly anisotropic, layered structure of the $\text{K}_4\text{Nb}_6\text{O}_{17}$ defines the shape of the cubic KNbO_3 crystallites.

Acknowledgment. We thank Dr. Marjan Bele, National Institute of Chemistry, Ljubljana, Slovenia, for SEM images. The work was financially supported by the Ministry of Higher Education, Science and Technology of Slovenia.

CM050079C

(18) Seno, Y.; Tani, T. *Ferroelectrics* **1999**, 224, 365.

(19) Kimura, T.; Yoshimoto, T.; Iida, N.; Fujita, Y.; Yamaguchi, T. *J. Am. Ceram. Soc.* **1989**, 72, 85.
 (20) Kimura, T.; Holms, M. H.; Newnham, R. E. *J. Am. Ceram. Soc.* **1982**, 65, 223.
 (21) Tani, T. *J. Korean Phys. Soc.* **1998**, 32, 1217.
 (22) Takeuchi, T.; Tani, T.; Saito, Y. *Jpn. J. Appl. Phys.* **1999**, 38, 5553.
 (23) Sugawara, T.; Shimizu, M.; Kimura, T.; Takatori, K.; Tani, T. *Ceram. Trans.* **2003**, 136, 389.
 (24) West, D. L.; Payne, D. A. *J. Am. Ceram. Soc.* **2003**, 86, 769.